Nanoscale

Accepted Manuscript

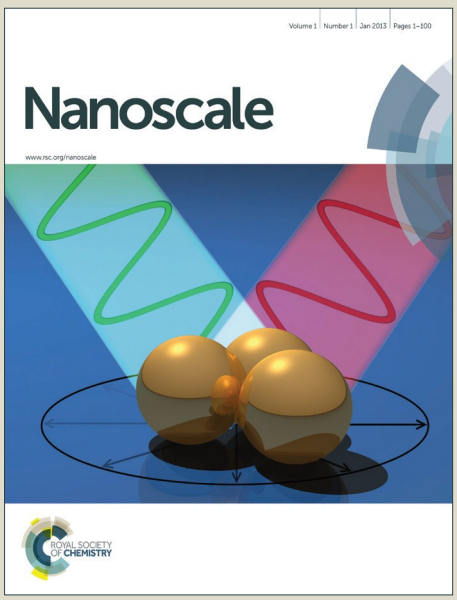

ROYAL SOCIETY OF CHEMISTRY

www.rsc.org/nanoscale

Journal Name

ARTICLE

Novel self-assembled sandwich nanomedicine for NIR-responsive release of NO

Received 00th January 20xx,
Accepted 00th January 20xx

DOI: 10.1039/x0xx00000x

www.rsc.org/

Jing Fan,[a,c,d] Qianjun He,*[b] Yi Liu,[d] Ying Ma,[d] Xiao Fu,[d] Yijing Liu,[d] Peng Huang,[d] Nongyue He*[a] and Xiaoyuan Chen*[d]

A novel sandwich nanomedicine (GO-BNN6) for near-infrared (NIR) light responsive release of nitric oxide (NO) has been constructed by self-assembling of graphene oxide (GO) nanosheets and a NO donor BNN6 through the π-π stacking interaction. GO-BNN6 nanomedicine has an extraordinarily high drug loading capacity (1.2 mg BNN6 per mg GO), good thermal stability, and high NIR responsiveness. The NO release from GO-BNN6 can be easily triggered and effectively controlled by adjusting the switching, irradiation time and power density of NIR laser. The intracellular NIR-responsive release of NO from GO-BNN6 nanomedicine causes a remarkable anti-cancer effect.

Introduction

Nitric oxide (NO) is a lipophilic, highly diffusible and short-lived free radical molecule which can be synthesized *in vivo* by the oxidation of L-arginine under the catalysis of nitric oxide synthase (NOS) enzymes. Molecular and nitrogenous free radical derivatives of NO, *e.g.* NO_2, NO_2^- and $ONOO^-$, can play a role as messengers for signaling the reactive nitrogen signal pathway to modulate biofunctions.[1] Especially in oncology research, tumor growth can be inhibited by increasing the level of NO, which was initially observed in macrophages mediated cytotoxicity.[2] On the other hand, too low level of NO can accelerate tumor angiogenesis.[3] In addition, NO is also able to reverse plasma-membrane P-glycoprotein (P-gp) transporters mediated multidrug resistance (MDR).[4]

Many NO donors have been developed for anti-tumor research, such as *N*-nitrosamines, metal NO complexes, Roussin's black salt (RBS), bis-*N*-nitroso compounds (BNNs) and so on. However, NO release from these donors is either spontaneous or only responsive to UV/Visible light (such as BNNs).[5] The spontaneous release lacks controllability and therefore has a potential risk of NO poisoning, while UV/Visible light has limited tissue penetrability and is also prone to phototoxicity, thus restricting the application of photo-responsive donors. By comparison, near-infrared (NIR) light has a higher depth of tissue penetration and a lower phototoxicity than UV light. Therefore, the NIR-responsive nanomedicine for controlled NO release is highly desired.

Some nanoparticles have been developed as carriers of NO donors for NO delivery and controlled release.[6] Ellen *et al.*[6c] covalently grafted silica nanoparticles with a NO donor, sodium 1-(pyrrolidin-1-yl)diazen-1-ium-1,2-diolate (PYRRO), on to with for therapy of ovarian cancer. However, the release of NO from PYRRO-Silica was spontaneous and thus had poor controllability. Recently, Zhao *et al.*[6a,b] used upconversion nanoparticles to mediate the NIR-triggered NO release from loaded RBS. This nanomedicine had some distinct advantages including good NIR-responsiveness and remarkable anti-MDR efficacy, but its drug loading capacity was poor and its photo-transferring efficiency (NIR-to-UV) was also low relatively. Therefore, more advanced NIR-responsive nanomedicine for NO controlled release is needed.

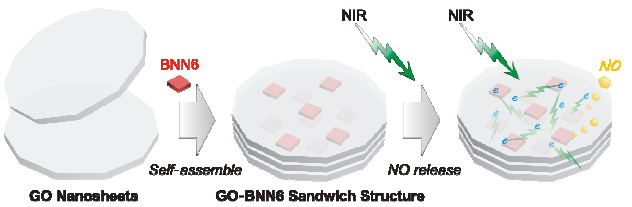

Scheme 1 Self-assembly and NIR-responsive mechanism of GO-BNN6 sandwich structure, which was assembled by GO nanosheets and BNN6 molecules through π-π stacking. The integrated sandwich structure of GO-BNN6 absorbs NIR light *via* GO and transforms photons into active electron from GO to caged BNN6 (green lightning), and then excites BNN6 to decompose and release NO (yellow bubbles).

In this work, a novel NIR-responsive sandwich nanomedicine (GO-BNN6) is constructed by self-assembling graphene oxide (GO) nanosheets and BNN6 (N,N'-di-*sec*-butyl-N,N'-dinitroso-1,4-phenylenediamine) through π-π stacking, as illustrated in Scheme 1. GO can absorb NIR light

[a] *State Key Laboratory of Bioelectronics, Southeast University, Nanjing 210096, Jiangsu, P. R. China*
[b] *Guangdong Key Laboratory for Biomedical Measurements and Ultrasound Imaging, Department of Biomedical Engineering, School of Medicine, Shenzhen University, Shenzhen 518060, Guangdong, P. R. China*
[c] *Clinical Laboratory, Nanxishan Hospital of Guangxi Zhuang Nationality Autonomous Region, Guilin 541002, Guangxi, P. R. China*
[d] *Laboratory of Molecular Imaging and Nanomedicine (LOMIN), National Institute of Biomedical Imaging and Bioengineering (NIBIB), National Institutes of Health (NIH), Bethesda, MD 20892, USA*

Electronic Supplementary Information (ESI) available: NMR and MS data of BNN6, stability of GO-BNN6, NIR-responsibility comparison of BNN6 and GO-BNN6, and NMR spectrum of RBSP. See DOI: 10.1039/x0xx00000x

and transform photons into active electrons from GO to caged BNN6 and then excite BNN6 to decompose and release NO effectively. Owing to the specific sandwich structure, GO-BNN6 exhibit an extraordinarily high drug loading capacity (1.2 mg BNN6 per mg of GO), and high NIR responsiveness and controllability for NO release. Furthermore, the intracellular NIR-responsive release of NO from GO-BNN6 causes remarkable anti-cancer effect.

Results and discussion

Synthesis and characterization of BNN6

Pacheco *et al.*[7] synthesized BNN5, a soluble NO donor, by adding a water-soluble *p*-phenylenediamine and nitric acid. Here we modified the method to synthesize water-insoluble BNN6 in an aqueous reaction system by using a kind of water-insoluble *p*-phenylenediamine (BPA, N,N'-bis-*sec*-butylamino-*p*-phenylenediamianne) as reactant, as shown in Fig. S1A. The reaction was facile as the red oil-like liquid BPA quickly became a beige solid BNN6 (Fig. S1A) once hydrochloric acid was added into the reaction system. The synthesized BNN6 was purified by washing with EtOH and drying under vacuum, and then characterized by ^{1}H NMR and MS. The ^{1}H NMR spectrum (Fig. S1B) indicated that two NO had replaced two hydrogen atoms on the *p*-phenylenediamine of BPA, forming the NO-caged structure of BNN6, as illustrated in Fig. S1A. The MS data further suggested that the molecular weight of synthesized BNN6 is 279 Dalton in accordance with the molecular structure of BNN6 (Fig. S1C). These results accordingly confirmed the success in the synthesis of BNN6. Furthermore, we confirmed that the photo-responsiveness of synthesized BNN6 to UV light. As shown in Fig. S1D, the light yellow solution of BNN6 in DMSO quickly became red once irradiated by UV light (365 nm), suggesting the photochemical degradation of BNN6 into NO and BHA. This indicated that synthesized BNN6 indeed has a UV-responsive decomposition profile that is similar to BNN5 with a similar NO-caged molecular structure.[8]

Synthesis and characterization of GO-BNN6 nanomedicine

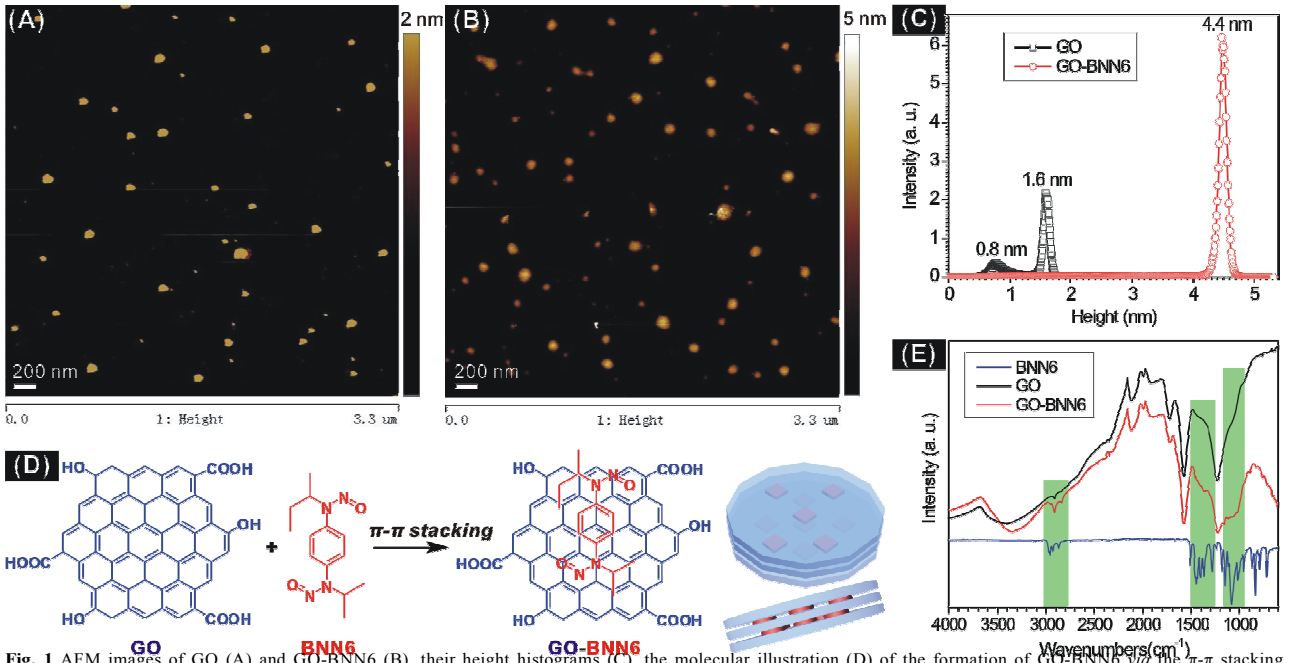

Fig. 1 AFM images of GO (A) and GO-BNN6 (B), their height histograms (C), the molecular illustration (D) of the formation of GO-BNN6 via the π-π stacking between GO and BNN6, and FT-IR spectra (E) of GO, BNN6 and GO-BNN6 where three green areas indicate the characteristic bands of BNN6.

GO was synthesized according to Liu's method.[9] From AFM data as shown in Fig. 1A-C, synthesized GO has a sheet-like morphology with about 100 nm in diameter (Fig. 2A) and 0.8 nm or 1.6 nm in thickness (Fig. 1C). This suggested that the synthesized GO consists of both single-layered and double-layered GO nanosheets. After assembly with BNN6, the diameter of GO-BNN6 remained almost unchanged (Fig. 1B), but the thickness of GO-BNN6 was increased to 4.4 nm. This indicated that GO and BNN6 self-assembled a sandwich structure with 3~4 layers of GO nanosheets in a single GO-BNN6 particle through the π-π attraction between them, as illustrated in Fig. 1D. Although GO-BNN6 was washed for more than 7 times with a DMSO/H_2O (50%:50%) solution, it could still maintain this sandwich structure and dimensions in water, indicating that GO-BNN6 was a stable complex in water. High dispersibility of GO-BNN6 in water suggested that the sandwich structure of GO-BNN6 remarkably improved the water solubility of highly hydrophobic BNN6 owing to the excellent hydrophilicity of synthesized GO. Since BNN6 is highly hydrophobic, the hydrophobic interaction between BNN6 and the hydrophobic zone of the GO nanosheet (as shown in Fig. 1D) also possibly made partial contribution to the self-assembly for GO-BNN6 besides the π-π attraction. Moreover from FTIR spectra (Fig. 3), it can be found that GO-

BNN6 exhibited the characteristic peaks of BNN6 (green bands) and GO, indicating that the synthesized GO-BNN6 nanomedicine is indeed the complex of BNN6 and GO. In addition, the aqueous solution of GO-BNN6 nanomedicine had a high stability as there was no visible decomposition after storing at room temperature in dark for 7 days (Fig. S2).

Moreover, the BNN6-loading capacity of GO-BNN6 was measured to be as high as 1.2 mg of BNN6 per mg of GO, which should be attributed to highly effective π-π interaction between GO and BNN6. Recently, Zhang and Garcia *et al*. used a core-shell structure of UCNP@MSN as carrier of RBS to develop a NIR-responsive nanomedicine (UCNP@MSN-RBS) for NO controlled release.[6a,b] How, the saturated RBS loading capacity of UCNP@MSN was merely 10wt%. In comparison, the developed sandwich structure of GO-BNN6 in this work has a remarkably higher drug loading capacity (120wt%). Such a high drug loading capacity will favor the decrease of carrier dosage and the duration of NO release per nanoparticle, consequently enhancing drug efficacy and lowering toxic side effects, which is highly desired in engineering high-performance anti-cancer nanomedicines.[10]

NIR-responsive release profiles of GO-BNN6 nanomedicine

The responsivity of GO-BNN6 nanomedicine to NIR light was investigated firstly. The NO concentration in PBS was measured using a Griess kit and a RBSP (Rhodamine B Spirolactam-based Probe) fluorescence probe (Fig. S3A). It can be found that BNN6 was not responsive to NIR light (808 nm), but to UV light (365 nm) for NO release (Fig. S3B and Fig. 2A), probably because its adsorption band mainly locates in the UV region rather than in the NIR region. By comparison, after BNN6 was stacked with GO, GO-BNN6 nanomedicine became sensitive to NIR light for NO release (Fig. S3B and Fig. 2A), and was also remarkably stable in the PBS solutions of pH=7.4 and 5.5 in the absence of NIR irradiation (Fig. S4). This indicates that GO plays a key role in the NIR-responsive NO release from GO-BNN6 nanomedicine. It has been proven that graphene has a photoelectronic effect, where the photo-induced electron/curent is generated on a single graphene nanosheet under excitation of light with different wavelengths from visible to infrared regions.[11a–c] Johannsen *et al.* have further discovered that graphene can effectively convert a single photon into multiple electrons.[11d] Recently, we have empolyed the photoelectronic effect of GO to convert NIR light into electrons for the degradation of caged metal carbonyl and the NIR-responsive on-demand release of CO successfully.[12] Therefore, we think that GO-BNN6 can also transform NIR photons into active electrons. Further, the sandwich structure of GO-BNN6 favors the transferring of active electrons on GO towards stacked BNN6 by a π-π approach, as illustrated in Scheme 1. These active electrons can therefore be utilized to excite BNN6 for photochemical decomposition of BNN6 and generation of NO (Scheme 1).

The mechanism for the photochemical decomposition and NO release of BNN-type NO donors (or BNNs) is that the photo-induced electrons excite the electron transfer along the aromatic ring and the detachment of two NO free radicals from one BNNs molecule.[13] The light absorption range of BNNs is limited in the UV region, and BNNs are therefore sensitive only to UV light, rather than NIR light. In this work, the developed sandwich structure of GO-BNN6 can absorb NIR light effectively, and transform photons into electrons, thus causing the decomposition of BNN6 into NO. Compared with BNNs, GO within GO-BNN6 seems like a NIR "antenna",[14] extending the function of the aromatic ring of BNNs.

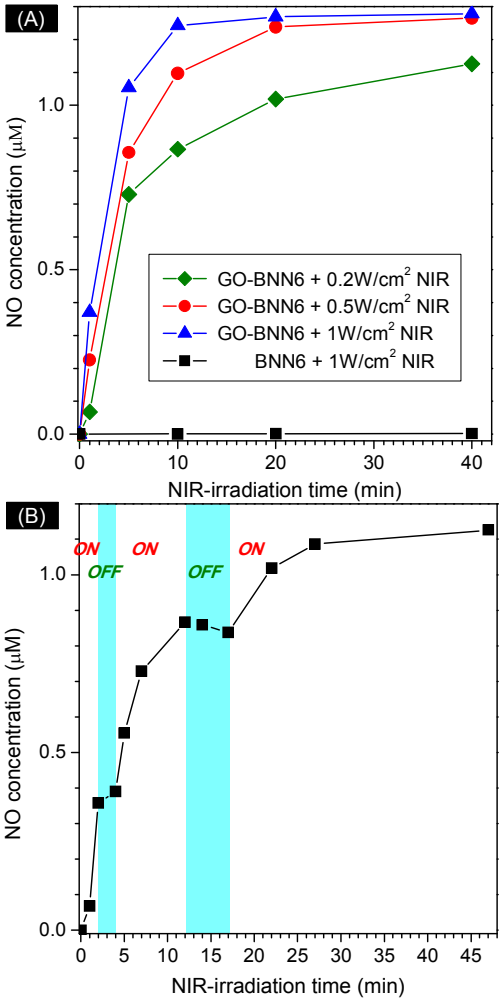

Fig. 2 (A) NO release profiles of GO-BNN6 nanomedicine in PBS under the excitation of 808-nm NIR light with different power densities (0.2, 0.5 and 1 W/cm²) measured by using a Griess kit; (B) the NIR controllability of GO-BNN6 nanomedicine for NO release by switching on/off 808-nm NIR light.

Furthermore, the NIR-responsive profiles of GO-BNN6 nanomedicine for NO release in the PBS was investigated under the excitation of 808-nm NIR light with different power densities. It could be found that GO-BNN6 nanomedicine was responsive to NIR light in a power density-dependent and irradiation time-dependent manner (Fig. 2A). It is very clear that more than half of NO can be quickly released from GO-BNN6 nanomedicine under excitation of 808-nm laser within several minutes, and then residual NO was released in a sustained way (Fig. 2A). This kind of drug release profile is thought to be quite useful for quickly achieving an effective

drug concentration for therapy and then maintaining the drug concentration within an effective but safe range. Moreover, higher power densities of NIR light caused faster release of NO from GO-BNN6 nanomedicine (Fig. 2A). Therefore, it is facile to control the NO release rate and amount by adjusting the NIR light power and/or NIR irradiation time. By increasing NIR light power and NIR irradiation time, GO can absorb more light energy to yield more electrons, and thus more quickly excite caged BNN6 to release NO.

The NIR controllability of GO-BNN6 nanomedicine for NO release was also investigated, as shown in Fig. 2B. When NIR light was switched on, the release of NO was initiated. Once NIR light was switched off, the release of NO stopped almost completely. The repeat of switching NIR light could also control NO release well in spite of decreased release rate with the increase of NIR irradiation time. This indicates that GO-BNN6 nanomedicine has an excellent NIR controllability for NO release. The NO concentration can be well controlled on demand through controlling the switching and power of NIR light, which is of great significance to manipulate the drug concentration within the therapeutic window and also reduce the risk of NO poisoning.

In addition, the influence of the photothermal effect of GO on NO release from GO-BNN6 nanomedicine was also investigated. As shown in Fig. 3, GO-BNN6 nanomedicine exhibited the photothermal effect compared with the blank control. The photothermal effect of GO-BNN6 depended on the power density of NIR light and the concentration of GO-BNN6. Higher power density of NIR light and higher concentration of GO-BNN6 led to stronger thermal effect (Fig. 3A). Among these sample groups, the greatest increase of temperature is 33°C after 20 min of NIR irradiaiton (200 μg/mL, 1.0 W/cm^2) with a final temperature of about 56°C. Direct heating to 60°C without NIR irradiation was used for comparison. It is clear that 1 min of direct heating at 60°C did not cause distinct NO release from GO-BNN6 nanomedicine, but 1 min of NIR irradiation at 1 W/cm^2 did lead to remarkable release of NO from GO-BNN6 nanomedicine (Fig. 3B). Temperature increase to 32.9°C in 1 min should not make contribution to the decomposition of GO-BNN6 nanomedicine as direct heating at 60°C did. Further increase of NIR-irradiation time to 20 min resulted in increased NO release, but the increase of direct heating time to 20 min at 60°C did not cause obvious NO release. Therefore, the NIR responsiveness of GO-BNN6 nanomedicine for NO release mainly derived from a photochemical decomposition effect of GO-BNN6 rather than the photothermal effect. In addition, we can suppress or enhance the photothermal effect by adjusting NIR irradiation time, NIR power density and GO-BNN6 concentration in order to avoid or combine the influence of thermal effect on NO therapy.

In order to demonstrate the photochemical conversion efficiency of GO-BNN6 nanomedicine for NO release, we compared it with another nanomedicine with a core-shell structure of BNN6-loaded gold nanorods@mesoporous silica nanoparticle (GNR@MSN-BNN6), which is similar to that of UCNP@MSN reported by Zhao.[6a,b] By comparison of their absorption spectra (Fig. 4A), it can be found that GO has a broad absorption band centered in the UV region, while GNR@MSN has a relatively narrow adsorption band centered in the NIR region. At the same concentration, GNR@MSN has higher absorbance at 808 nm than GO. But GO-BNN6 nanomedicine actually exhibited higher responsiveness to 808 nm NIR light compared with GNR@MSN-BNN6 nanomedicine in spite of NIR power density as more than 60% NO could be quickly released from GO-BNN6 nanomedicine after 5 min of NIR irradiation while the NO released percentage of GNR@MSN-BNN6 nanomedicine was less than 20% (Fig. 4B). This suggests that GO can more effectively transfer active electrons to loaded BNN6. Higher electron transferring efficiency of GO-BNN6 nanomedicine could be credited with its sandwich structure of the close π-π stacking between GO and BNN6.

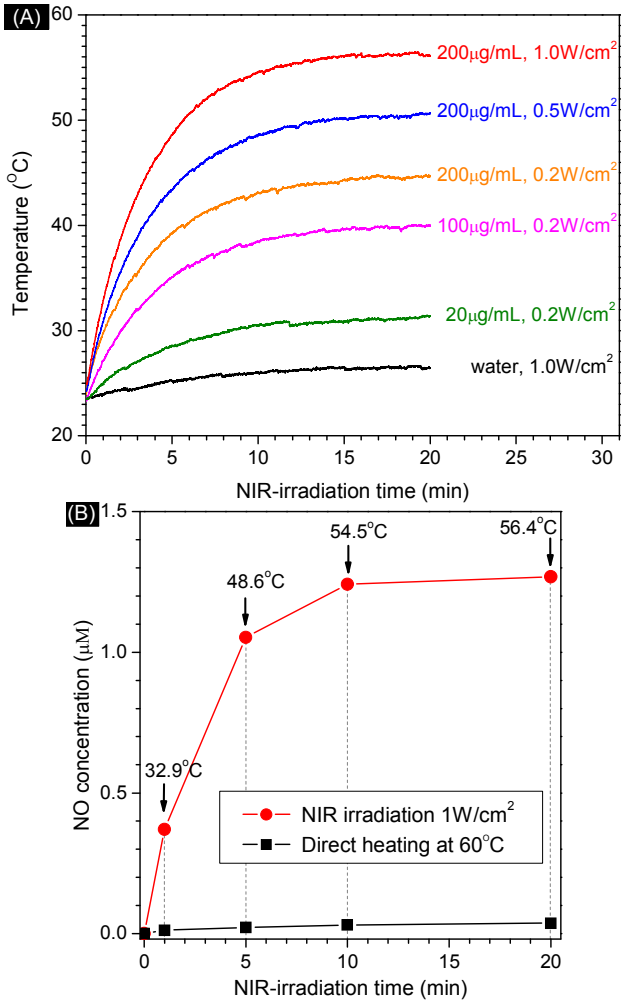

Fig. 3 Photothermal effect of GO-BNN6 at different concentrations (20, 100, 200 μg/mL) and under different NIR power densities (A), and the influence of NIR irradiation and direct heating on NO release from GO-BNN6 (B). In Fig. 3A, water without GO-BNN6 was used as blank control.

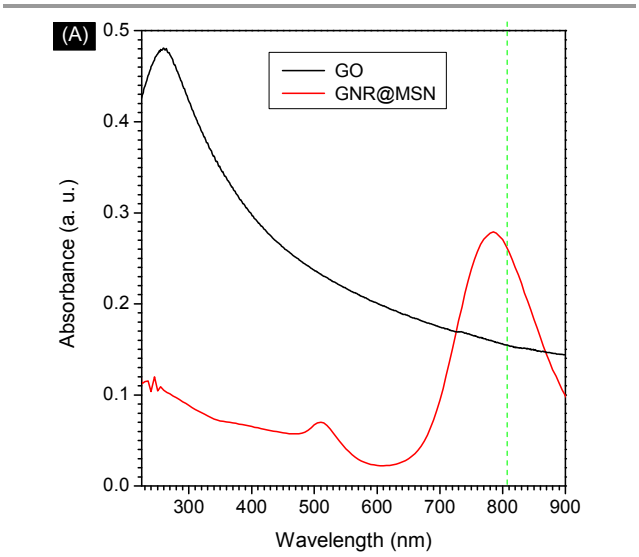

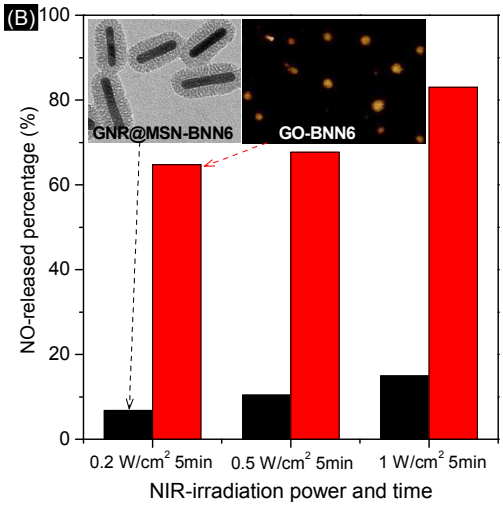

Fig. 4 Comparison of the adsorption spectra of GO and GNR@MSN at the same concentration (A), and comparison of the NIR-responsivity of GO-BNN6 and GNR@MSN-BNN6 nanomedicines for controlled release of NO at different power densities of NIR irradiation (B).

***In vitro* NIR-responsive release behavior and anti-cancer effect of GO-BNN6 nanomedicine**

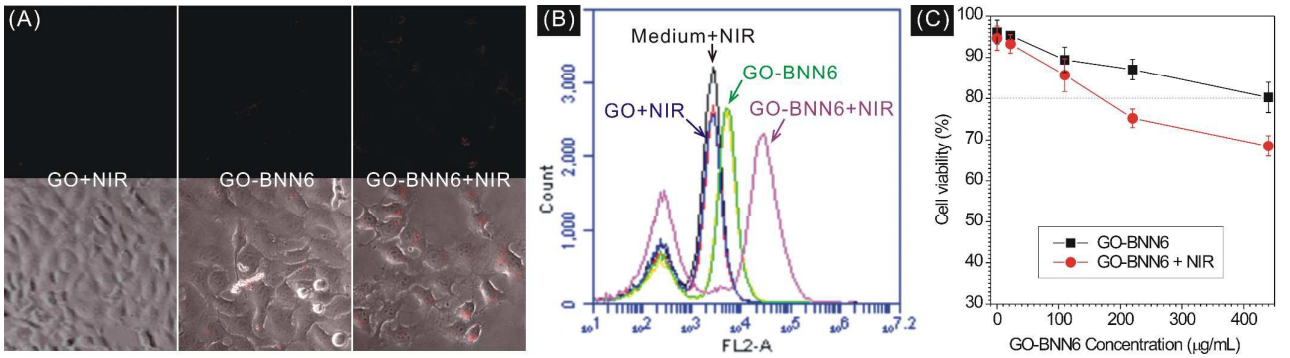

Fig. 5 Intracellular NIR-responsive NO release profiles of GO-BNN6 nanomedicine under the excitation of 808-nm NIR light detected with RBSP: (A) qualitative observation under fluorescence microscope; (B) flow cytometry statistics of the fluorescence intensity of treated 143B cells. (C) Cytotoxicity comparison of GO-BNN6 and GO-BNN6 plus NIR irradiation (808 nm NIR laser, 0.2 W/cm^2, irradiated 2 min) at different concentrations against 143B cells.

Intracellular NIR-responsive release profiles of GO-BNN6 nanomedicine were measured using RBSP fluorescence probe (Fig. S3A), which was synthesized according to Xue's method.[15] Human osteosarcoma 143B cells were chosen as a model cell line for the measurement of intracellular NIR-responsive NO release and anti-cancer effect of GO-BNN6 nanomedicine. After 2 h incubation with GO-BNN6 nanomedicine (100 μg/mL) and RBSP fluorescence probe (20 μM), residual nanoparticles and probe outside cells were washed off, and then treated 143B cells were irradiated under 808 nm NIR laser (0.2 W/cm^2) for 2 min. The determination of reasonable NIR irradiation parameters will depend on the balance between drug efficacy and toxic side effect. In order to avoid the side effects of NIR irradiation against cells as much as we can, we chose relatively low NIR irradiation power (0.2 W/cm^2) and short irradiation time (2 min) for cell experiments. From Fig. 5A, it could be found that large amounts of NO were released in 143 cells in the GO-BNN6+NIR group as suggested by intracellular red fluorescence. In the absence of NIR irradiation, there was negligible red fluorescence in cells in the GO-BNN6 group, indicating a low level of NO. Similarly, the GO+NIR group as a control also had no distinct NO signal. Therefore, these low levels of NO were thought to be possibly derived from cells rather than nanomedicine, and could therefore be considered as background. Furthermore, the fluorescence intensity of treated 143B cells was quantified by flow cytometry (Fig. 5B). The statistics results also indicated that the GO-BNN6+NIR group exhibited remarkably stronger fluorescence signal as compared to other groups. These results consistently indicated that GO-BNN6 can responsively release NO in cells under NIR irradiation.

Furthermore, the cytotoxicity of GO-BNN6 nanomedicine against 143B cells was investigated (Fig. 5C). In the absence of NIR irradiation, GO-BNN6 nanomedicine exhibited a weak cytotoxicity against 143B cells as more than 80% cells remained viable at GO-BNN6 concentration of as high as 440 μg/mL, suggesting relatively good biocompatibility. However after NIR irradiation (0.2 W/cm^2) for only 2 min and then incubation for 16 h, GO-BNN6 nanomedicine always killed more 143B cells regardless of GO concentration, suggesting a remarkable NIR-responsive anti-cancer effect. Moreover, the anti-cancer effect depended on the concentration of GO-BNN6

nanomedicine. At higher concentration of GO-BNN6, the difference of cytotoxicity between GO-BNN6 and GO-BNN6+NIR groups became more distinguished, possibly owing to more uptake of GO-BNN6 nanomedicine by cells and thus more NO release in cells under the NIR triggering. Since the high intracellular level of NO can kill cancer cells,[3] the anti-cancer effect of GO-BNN6 should be mainly derived from the intracellular NIR-responsive release and accumulation of NO.

Experimental

Synthesis and characterization of BNN6

N,N'-Di-sec-butyl-N,N'-dinitroso-1,4-phenylenediamine (BNN6) was synthesized with an addition reaction as following. 2.34 mL (10 mmol) N,N'-bis-*sec*-butylamino-*p*-phenylenediamianne (BPA, TCI America Inc.) was diluted into 18 mL ethanol, and then 20 mL 6 M degassed aqueous solution of $NaNO_2$ (Sigma-Aldrich) was added under stirring and under nitrogen protection. After 30 min, 20 mL 6M aqueous solution of HCl was added dropwise using a separating funnel. The reaction solution gradually became orange from red, and meanwhile a beige precipitation yielded. After stirring for 4 h, the solid product was collected by centrifugation, and the collected precipitate was washed with water and 50% (v/v) ethanol/water in turn several times to remove residual reactants, and then dried under freezing vacuum in dark environment overnight. The structure of synthesized BNN6 was confirmed by Hydrogen Nuclear Magnetic Resonance (^{1}H NMR, Bruker Magnet System, 300 MHz/54 mm) and Mass Spectrum (MS, Waters LC-MS System, Milford, MA) measurements. ^{1}H NMR (300 MHz, $CDCl_3$): δ 7.52 (4H), 4.95-4.69 (2H), 2.00-1.84 (2H), 1.81-1.69 (2H), 1.48 (t, J=7.6 Hz, 6H), 1.08 (td, J=7.4, 5.3 Hz, 6H). MS (ESI+): calcd. for $C_{14}H_{22}N_4O_2$, 278.2 $[M]^+$; found 279.2 $[M]^+$.

Construction and characterization of GO-BNN6 nanomedicine

GO-BNN6 nanomedicine was constructed by a facile self-assembly route. GO nanosheets were firstly synthesized according to Yang's protocol.[9] GO (4.2 mg) was resuspended in 4 mL DMSO under stirring, and then a DMSO solution of BNN6 (1 mL, 8.4 mg/mL) was dropwise added. Keep stirring in dark for 12 h to mix GO and BNN6 fully, and then keep static for 2 h to allow their self-assembly. The mixture solution was diluted with 5 mL water to allow the filtration of nanoparticles by an Amicon® centrifugal filter device (molecular weight cutoff: 10 K). The separated nanoparticles were washed with excess water to remove residual BNN6 and DMSO, and then dispersed into 5 mL water for storing. All the filtered/washing solutions were collected to calculate the loading capacity according to the Beer-Lambert law and UV absorbance measurement (Genesys 10S UV-Vis spectrophotometer, Thermo Sci.).

Morphologies of GO and GO-BNN6 were characterized by Atomic Force Microscope (AFM). Diluted aqueous solutions of GO-BNN6 and GO were deposited on clean mica, and then dried by blowing away the excess fluid with nitrogen gas. The dried samples were sealed into the sample compartment dehumidified by Drierite® particles, and then imaged with a gentle tapping mode by a PicoForce Multimode 8 AFM (Bruker, CA). The collected AFM images were further processed to obtain dimensional histograms with the Nanoscope® software (version 7.3, Bruker, CA). The collected AFM images were further processed to obtain dimensional histograms with the Nanoscope® software (version 7.3, Bruker, CA).

Structures of GO and GO-BNN6 were characterized by attenuated total reflectance Fourier transform infrared spectroscopy (ATR-FTIR). Concentrated sample solutions were dropped on the universal diamond ATR sampling accessory and slowly dried by blowing with nitrogen gas. FT-IR spectra were then collected on a Thermo-Nicolet Nexus 670 ATR-IR spectrometer.

Measurement of stability of GO-BNN6 nanomedicine

The UV spectrum of a freshly prepared aqueous solution of GO-BNN6 (0.7 mg/mL) was measured. The solution was put at room temperature in a light-sealed environment. After 7 d, the UV spectrum of the solution was collected again. The stability of GO-BNN6 could be confirmed by checking the difference of UV spectra before and after 7 d.

Detection of NO release in the aqueous solution with a Griess kit

A commercial Griess assay kit (Promega Corporation, USA) was used to detect the release of NO from BNN6 and GO-BNN6 nanomedicine. The instruction method was modified as follows to meet our instruments and obtain a lower limit of detection. 100 μL of sample was mixed with 100 μL of the sulfanilamide solution (1% sulfanilamide in 5% phosphoric acid), and then the mixed solution was shake for 10 min at room temperature in dark. Then 100 μL of the NED solution (0.1% N-1-napthylethylenediamine dihydrochloride in water) was added to incubate 10 min at room temperature in a light-sealed environment. Finally, the mixture was diluted with 200 μL water for UV spectrophotometer measurement. In order to eliminate the effect of GO, the GO nano-composites were removed from the GO-BNN6 samples after NIR exposure (808 nm laser) by centrifugation at a speed of 20,000*g*. The supernatant was collected for measurement by following the modified Griess method. $NaNO_2$ standard samples (0.05 μM ~ 25 μM) were used to establishing a standard curve for calculation of NO concentrations.

NIR laser irradiation (808 nm) at different power densities of 0.2, 0.5 and 1 W/cm^2 was used to trigger the NO release from BNN6 and GO-BNN6 nanomedicine. By comparison, UV light (365 nm) was also used to trigger the release of NO from BNN6. The amount of released NO was detected by the above-mentioned Griess method. In addition, an infrared thermal imaging device (FLIR® Systems, Inc.) was used to measure the change in temperature of sample solutions with time under NIR irradiation.

Detection of intracellular NO release with the RBSP fluorescence probe and by flow cytometry

Firstly, the RBSP fluorescence probe based on rholdamine B (RhB) was prepared according to Xue's method as the following.[15] To a solution of RhB (192 mg, 0.4 mmol) in 20 mL chloroform, *o*-phenylenediamine (864 mg, 8 mmol) and (benzotriazol-1-yloxy)tripyrrolidinophosphonium hexafluorophosphate (208 mg, 0.4 mmol) were added to obtain a red solution. The mixture was stirred at room temperature for 24 h under N_2 protection to form a yellow solution. Then the solvent was removed under reduced pressure, the yellow powder product was purified by the silica column (ethyl acetate/hexane, v/v, 1:1) to obtain the white power in the yield of 70%. The structure of the product RBSP was confirmed by ^{1}H NMR (300 MHz, $CDCl_3$): δ 8.03 (d, J = 6.1 Hz, 1H), 7.60 – 7.50 (m, 2H), 7.23 (s, 1H), 6.95 (t, J = 7.4 Hz, 1H), 6.64 (d, J = 8.7 Hz, 2H), 6.55 (d, J = 8.3 Hz, 1H), 6.41 (t, J = 7.5 Hz, 1H), 6.31 (d, J = 9.1 Hz, 2H), 6.26 (s, 2H), 6.09 (d, J = 7.9 Hz, 1H), 3.32 (q, J = 7.1 Hz, 8H), 1.14 (t, J = 7.0 Hz, 12H) (Fig. S5).

The DMSO solution of RBSP (10 mM) was diluted 500 times with cell culture medium under shaking. 143B cells (5×10^3) were seeded on a slide. The RBSP solution (20 μM) and the GO-BNN6 solution (100 μg/mL) were added. After incubation for 2 h, cells were washed with PBS to remove residual RBSP and nanoparticles, and then were irradiated under 0.2W/cm^2 NIR laser for 2 min. The slides were put back into incubator. After 8 h of incubation, cells were imaged on a confocal fluorescence microscope. Moreover, cells were also collected for statistics of the fluorescence intensity by flow cytometry.

In order to investigate the stability of GO-BNN6 at tumor microenvironment and under physiological conditions, two GO-BNN6 samples were incubated respectively in pH 7.4 and 5.5 PBS solutions at 37°C in the absence of NIR irradiation for 40 min. The Griess assay was used to detect NO release.

Synthesis and characterization of GNR@MSN carrier and GNR@MSN-BNN6 nanomedicine

GNRs with the strongest absorption peak at 780 nm were synthesized according to Xia's method.[16] The growth solution was prepared as, $HAuCl_4$ (0.01 M) 9 mL, silver nitrate (0.02 M) 1.1 mL, hydroquinone (0.33 M) 3.6 mL were sequentially added into 210 mL of CTAB (0.11 M) solution under slight mixing. After standing for 5 min, 0.75 mL $NaBH_4$ (0.498 mM) solution was added and kept standing in 30°C over 12 h. Then mesoporous silica was coated on GNRs according to the following method. 50 mL GNRs were washed with water for 2 times and then re-dispersed into 10 mL water. 30 μL ammonium hydroxide (30%) was added and the mixture was stirred 1 h at 40°C. Dropwise add 100 μL 2.5% EtOH solution of TEOS, keep stirring 24 h, and wash with water and EtOH to remove CTAB in turn. The prepared GNR@MSN was mixed with 100 mg/mL BNN6 solution in DMSO, and the mixture solution was shake overnight. GNR@MSN-BNN6 nanoparticles were collected by centrifugation, washed with water and used for NIR-responsive release experiments.

Measurement of cytotoxicity of GO-BNN6 nanomedicine

Cell viabilities of 143B cells treated with GO-BNN6 nanomedicine and GO-BNN6 plus NIR irradiation were determined by the colorimetric MTT method. 143B cells were seeded in 96-well plate at a density of 2×10^4 cells per well, and incubated overnight at 37 °C in 5% CO_2 atmosphere. After being washed with PBS (pH 7.4), the cells were incubated with 100 μL GO-BNN6 nanomedicine at different concentrations (0, 22, 110, 220 and 440 μg/mL) at 37 °C for 2 h under the same conditions. Then all cells were rinsed with PBS and incubated 12 h in MEM at 37°C in 5% CO_2 atmosphere. Cells were exposed under 808 nm NIR laser with a power density of 0.2 W/cm^2 for 2 min, and then cell plates were put back to incubator. After 16 h of incubation, medium was replaced with 100 μL 0.5 mg/mL MEM solution of MTT. After 2 h, the medium was removed and 100 μL of DMSO was added in each well to completely dissolve the crystals. The absorbance at 570 nm was recorded by a microplate reader. The cytotoxicity was expressed as the percentage of cell viability as compared with the blank control. Each data point was represented as a mean ± standard deviation of eight independent experiments (n = 8).

Conclusions

BNN6 as a NO donor has been successfully synthesized. GO-BNN6 nanomedicine has been successfully constructed with GO nanosheets and BNN6. The constructed GO-BNN6 nanomedicine has a novel sandwich structure, high thermostability and excellent dispersion in water. The NO release is measured using a Griess kit and a RBSP fluorescence probe, suggesting a high NIR-responsiveness and controllability of GO-BNN6. Through adjusting the switching, irradiation time and power density of NIR laser, the release of NO from GO-BNN6 nanomedicine has been well controlled. The *in vitro* anti-cancer cell experiments have indicated that the GO-BNN6 nanomedicine could release NO in cancer cells under the irradiation of NIR light, and thus inhibited the growth of 143B cancer cells effectively. This advanced nanomedicine is hopefully applied for NO therapy of cancer.

Acknowledgements

We thank the financial support from the Intramural Research Program, National Institute of Biomedical Imaging and Bioengineering, National Institutes of Health, the National Key Program for Developing Basic Research of Chinn (No. 2014CB744501), the NSFC (Nos. 61271056, 61471168 and 61527806), and the State Scholarship Fund from China Scholarship Council (No. 201406090085).

Notes and references

1 R. SoRelle, *Circulation*, 1998, **98**, 2365–2366.
2 (a) D. J. Stuehr and M. A. Marletta, *P. Natl. Acad. Sci. USA*, 1985, **82**, 7738–7742; (b) J. B. Hibbs, R. R. Taintor, Z. Vavrin

and E. M. Rachlin, *Biochem. Biophy. Res. Commun.*, 1988, **157**, 87–94.
3 W. Xu, L. Liu, M. Loizidou, M. Ahmed, I. G. Charles, *Cell Res*., 2002, **12**, 311–320.
4 (a) M. F. Chung, H. Y. Liu, K. J. Lin, W. T. Chia and H. W. Sung, *Angew. Chem.*, 2015, **127**, 10028–10031; (b) A. de Luca, N. Moroni, A. Serafino, A. Primavera, A. Pastore, J. Z. Pedersen, R. Petruzzelli, M. G. Farrace, P. Pierimarchi, G. Moroni, G. Federici, P. S. Vallebona and M. L. Bello, *Biochem. J.*, 2011, **440**, 175–183; (c) C. P. Muir, M. A. Adams and C. H. Graham, *Breast Cancer Res. Tr.*, 2006, **96**, 169–176.
5 J. Kim, G. Saravanakumar, H. W. Choi, D. Park and W. J. Kim, *J. Mater. Chem. B*, 2014, **2**, 341–356.
6 (a) X. Zhang, G. Tian, W. Yin, L. Wang, X. Zheng, L. Yan, J. Li, H. Su, C. Chen, Z. Gu and Y. Zhao, *Adv. Funct. Mater.,* 2015, **25**, 3049–3055; (b) J. V. Garcia, J. Yang, D. Shen, C. Yao, X. Li , R. Wang, G. D. Stucky, D. Zhao, P. C. Ford and F. Zhang, *Small,* 2012, **8**, 3800–3805; (c) X. F. Zhang, S. Mansouri, D. A. Mbeh, L'H. Yahia, E. Sacher and T. Veres, *Langmuir*, 2012, **28**, 12879–12885; (d) D. Ostrowski, B. F. Lin, M. V. Tirrell and P. C. Ford, *Mol. Pharm.* 2012, **9**, 2950–2955; (e) E. V. Stevens, A. W. Carpenter, J. H. Shin, J. Liu, C. J. Der and M. H. Schoenfisch, *Mol. Pharm.*, 2010, **7**, 775–785.
7 M. Z. Cabail, P. J. Lace, J. Uselding and A. A. Pacheco, *J. Photochem. Photobiol. A Chem.*, 2002, **152**, 109–121.
8 S. Namiki, F. Kaneda, M. Ikegami, T. Arai, K. Fujimori, S. Asada, H. Hama, Y. Kasuya and K. Goto, *Bioorg. Med. Chem.,* 1999, **7**, 1695–1702.
9 K. Yang, L. Feng, H. Hong, W. Cai and Z. Liu, *Nat. Protoc.*, 2013, **8**, 2392–2403.
10 (a) X. T. Zheng and C. M. Li, *Mol. Pharm*., 2012, **9**, 615–621; (b) Y. Lu, P. Wu, Y. Yin, H. Zhang and C. Cai, *J. Mater. Chem. B*, 2014, **2**, 3849–3859; (c) Q. He, Y. Gao, L. Zhang, Z. Zhang, F. Gao, X. Ji, Y. Li and Jianlin Shi, *Biomaterials*, 2011, **32**, 7711–7720; (d) Q. He and J. Shi, *J. Mater. Chem.*, 2011, **21**, 5845–5855.
11 (a) J. Park, Y. H. Ahn and C. Ruiz-Vargas, *Nano Lett*., 2009, **9**, 1742–1746; (b) T. Mueller, F. Xia and P. Avouris, *Nat. Photon*. 2010, **4**, 297–301; (c) N. M. Gabor, *Acc. Chem. Res*., 2013, **46**, 1348–1357; (d) J. C. Johannsen, S. Ulstrup, A. Crepaldi, F. Cilento, M. Zacchigna, J. A. Miwa, C. Cacho, R. T. Chapman, E. Springate, F. Fromm, C. Raidel, T. Seyller, P. D. C. King, F. Parmigiani, M. Grioni and P. Hofmann, *Nano Lett*., 2015, **15**, 326–331.
12 Q. He, D. O. Kiesewetter, Y. Qu, X. Fu, J. Fan, P. Huang, Y. Liu, G. Zhu, Y. Liu, Z. Qian and X. Chen, *Adv. Mater*., 2015, in press, DOI: 10.1002/adma.201502762.
13 (a) S. Namiki, T. Arai and K. Fujimori, *J. Am. Chem. Soc*., 1997, **119**, 3840–3841; (b) M. Yoshida, M. Ikegami, S. Namiki, T. Arai and K. Fujimori, *Chem. Lett*., 2000, **7**, 730–731; (c) M. Z. Cabail, P. J. Lace, J. Uselding, A. A. Pacheco, *J. Photochem. Photobiol. A*: *Chem*. 2002, **152**, 109–121.
14 S. Wecksler, A. Mikhailovsky and P. C. Ford, *J. Am. Chem. Soc*., 2004, **126**, 13566–13567.
15 Z. Xue, Z. Wu and S. Han, *Anal. Method.*, 2012, **4**, 2021–2026.
16 L. Zhang, K. Xia, Z. Lu, G. Li, J. Chen, Y. Deng, S. Li, F. Zhou and N. He, *Chem. Mater.*, 2014, **26**, 1794–1798.